ACADEMIC PRESS

Available online at www.sciencedirect.com
SCIENCE DIRECT®

Journal of Catalysis 218 (2003) 239–248

JOURNAL OF CATALYSIS

www.elsevier.com/locate/jcat

Optimization of zeolite Beta by steaming and acid leaching for the acylation of anisole with octanoic acid: a structure–activity relation

A.E.W. Beers,[a,*,1] J.A. van Bokhoven,[b,2] K.M. de Lathouder,[a] F. Kapteijn,[a] and J.A. Moulijn [a]

[a] *Section Industrial Catalysis, Delft University of Technology, Julianalaan 136, 2628 BL Delft, The Netherlands*
[b] *Department of Inorganic Chemistry, Utrecht University, Sorbonnelaan 16, Utrecht, The Netherlands*

Received 31 May 2002; revised 16 August 2002; accepted 16 September 2002

Abstract

This paper presents a catalytic and spectroscopic study of the dealumination of a commercial zeolite, Beta (Zeolyst). After dealumination by hydrochloric or oxalic acid and steaming (up to 973 K), increased activity and selectivity were found in the acylation of anisole with octanoic acid. The treatments led to the extraction of aluminum from the crystallographic T-sites in the framework structure, giving amorphous extraframework aluminum(–silicon)–oxide species in the case of steaming, while treatment with mineral acids or complexing agents removed framework and extraframework aluminum from the zeolite. ^{27}Al MQ MAS NMR revealed a changing of the aluminum coordinations and a shift from framework to extraframework species after steaming. Steaming removes aluminum from other crystallographic T-sites than acid leaching. Using nitrogen physisorption, no differences in the texture properties could be observed and XRD showed that the crystallinity was preserved, indicating high stability of the commercial zeolite Beta. The nature of the enhanced activity is suggested to result from higher accessibility of the active sites that are proposed to be associated with framework-connected aluminum atoms.

Keywords: Zeolite Beta; Dealumination; Acylation; ^{27}Al MQ MAS NMR

1. Introduction

The acylation of aromatics is the main route for the formation of aromatic ketones, which are important intermediates in the pharmaceutical, fragrance, flavor, and agrochemical industry. Conventionally, these reactions are catalyzed by metal halides (such as $AlCl_3$) or by strong mineral acids (such as HF and H_2SO_4). Problems associated with the metal halides as catalysts include the relatively strong complex formed between the ketone product and the metal chloride and the need to hydrolyze the complexes formed. "Catalysts" are therefore used in more than stoichiometric amounts. This leads to large corrosive waste streams, because the "catalyst" cannot be regenerated. This type of "catalyst" should rather be seen as a reactant; moreover, halide-containing side-products are formed. The use of a solid acid catalyst can overcome these disadvantages [1]. These catalysts can be separated from the reaction mixture and reused. Besides, these "green" materials are not harmful to the environment, because they are not corrosive and do not produce corrosive side-products. Different types of materials can be considered for their applicability as solid acid catalysts. Examples are zeolites and ion-exchange resins.

In the fine chemical industry, solid acids are generally used as slurry catalysts in batch reactors. The main disadvantage of using these materials in liquid phase reactions is the laborious and expensive separation of the catalyst particles from the reaction mixture. Also, due to the high stirring speed for mixing, attrition of the particles occurs. By fixing the catalyst in the reactor, for example in a fixed bed, separation is not necessary any more. The disadvantage of a fixed bed, however, is that the particle size of the catalyst is increased to prevent pressure drop issues, leading to lower catalyst effectiveness and (depending on the kinetics) lower selectivity. By integration of the catalyst with the reactor using a structured support, separation and attrition problems are circumvented, so the catalyst can be used for a longer

* Corresponding author.
E-mail addresses: annemarie.beers@engelhard.com (A.E.W. Beers), j.a.vanbokhoven@tech.chem.ethz.ch (J.A. van Bokhoven).
[1] Present address: Engelhard, PO Box 19, 3454 ZG De Meern, The Netherlands.
[2] Present address: Laboratory for Technical Chemistry, ETH Hönggerberg, CH-8093 Zurich, Switzerland.

0021-9517/03/$ – see front matter
doi:10.1016/S0021-9517(03)00022-8

period. Coating the walls of a structured reactor with a thin layer of catalyst leads to high effectiveness and selectivity by reducing diffusional distances. Furthermore, depending on the shape of the structure, the pressure drop decreases toward zero [2].

In the literature, a large number of zeolite catalysts have been described as active catalysts in the acylation of aromatics. The most common zeolites for acylation are Y (mostly dealuminated), Beta, and MFI [3–7]. In the acylation of toluene and xylene with carboxylic acids, performed in the liquid phase (200 °C, 48 h), rare-earth-modified zeolites were used as catalysts [8–10]. In an industrial process by Rhodia Chimie [11], the acylation of anisole and veratrole is performed with acetic anhydride in a recycle fixed bed reactor over zeolites FAU and BEA.

BEA and FAU are often reported to show higher activity than MFI [4,5,11]. Considering the 12-ring pores of BEA and FAU, comparable activities might be expected, but BEA often shows the highest activity, as in the acylation of anisole with acetic anhydride [4]. A way to improve the performance of a zeolite is by steaming and acid leaching. This is already done on a large scale to improve of the performance of other zeolites, such as zeolite MFI for octane boosting in the FCC process, zeolite Y or FAU to create ultrastable Y (USY) [13], and mordenite for the paraffin hydroisomerization process [14]. Possible reasons are the creation of active sites of enhanced activity, an increase in the number of active sites, and an enhancement in the accessibility of the active sites due to reduced diffusion limitations.

Steaming and acid leaching treatments are well known to cause dealumination of zeolite structures, that is, removal of aluminum atoms from the framework. Dealumination of a BEA zeolite is reported to occur very easily [15]. Dealumination during calcination in deep beds is a kind of "in situ steaming," due to water produced in the zeolite structure from template oxidation [16]. Dealumination as a result of treatment with oxalic acid is caused by strong coordination complexation with the aluminum cation. The oxalate ion forms stable complexes with almost any metal ion. The size of oxalic acid (0.29×0.54 nm) makes penetration of large zeolite pores possible and can therefore effectively remove aluminum from the lattice by forming a complex of an aluminum ion which is surrounded by one oxalate ion and water ligands. In this way, high $(\mathrm{Si/Al})_{\mathrm{bulk}}$ ratios (> 100) are obtained, even with treatment at room temperature [15]. During steam treatments the Si/Al ratio of the framework is increased, keeping the bulk ratio unchanged, since the Al is not removed.

The goal of this work is two-fold: (i) to develop a highly active and selective Beta zeolite as catalyst for the acylation of anisole with octanoic acid by means of steaming and acid leaching and (ii) to obtain an explanation for the change in activity and selectivity. To this end, Beta ($\mathrm{Si/Al} = 13$) is steamed at temperatures up to 973 K using different water partial pressures, and acid is leached by treatment in hydrochloric acids and oxalic acid. The effect of steaming and acid leaching of zeolite Beta on the activity in the acylation of anisole with octanoic acid is studied and compared with characterization by physicochemical analytical methods, such as XRD, N_2 physisorption, and ^{27}Al MQ MAS NMR. Deactivation in acylation is most likely due to sorption phenomena of reactants and products on the surface of the zeolite [17–20]. To enhance the performance of the zeolite in the acylation of aromatics catalytic reactor configurations in which these competitive adsorption effects are minimized, such as monolith type reactors, should be applied. As this paper represents a study of the correlation between the intrinsic activity of a catalyst and the structure of the zeolite, this aspect was not studied.

2. Experimentals and methods

2.1. Materials

Beta (bulk Si/Al 13) was purchased from Zeolyst International (CP 814 E-22) in the H^+-form. Hydrochloric acid was purchased from Merck, and oxalic acid was obtained from Baker.

2.2. Steaming and acid treatment procedure

Beta is steamed in a glass fixed-bed configuration with a diameter of either 2 or 5 cm and a bed height of 4 cm. Water is added by a liquid dosage pump and evaporates during transport through the tube to the reactor. The water vapor fraction was varied from 30 to 72 vol% in Ar; the steaming temperature and time were varied from respectively 673–973 K and 1 to 24 h. The acid leaching procedure includes treating Beta (5 g) in 100 ml of either 1 M hydrochloric acid or 1 M oxalic acid under stirring. Table 1 summarizes the treatments and sample codes.

2.3. Characterization

Nitrogen physisorption measurements (for micro- and mesopore analysis) were carried out with a Quantachrome Autosorb-6P at 77 K. Pore volume and pore size distribution were calculated using the Brunauer–Emmett–Teller (BET) model.

TEM was done on a Philips CM30T electron microscope with a LaB_6 filament as the source of electrons, operated at 300 kV. Samples were mounted on a Quantifoil microgrid carbon polymer, supported on a copper grid.

XRD was done on a Philips PW1840 diffractometer, equipped with a PW 1830 generator.

XRF was performed on a Philips PW1480.

^{27}Al multiple quantum magic angle spinning nuclear magnetic resonance (^{27}Al MQ MAS NMR) was used to determine the coordination of the aluminum in the zeolite samples. With this technique pure isotropic spectra with high

Table 1
Steaming and acid treatment procedures to Beta

	T (K)	H_2O (Vol%)	Time (h)	Acid	Time (min)	BET SA (m^2/g)	Bulk Si/Al ratios as determined with XRF (–)
P (parent)	–	–	–	–	–	640 ± 20	6.5
1	673	38	1	–	–	600 ± 20	
2	673	38	2	–	–	610 ± 20	6.5
3	673	38	3	–	–	610 ± 20	6.5
4	673	38	10	–	–		6.6
5	673	38	24	–	–		6.5
6	723	72	4	–	–	613 ± 5	
7	923	72	4	–	–		
8	973	72	4	–	–		6.7
9	673	42	1	Hydrochloric acid[a]	45	651 ± 5	11.7
10	673	42	2	Hydrochloric acid[a]	45	649 ± 5	11.3
11	673	42	3	Hydrochloric acid[a]	45	649 ± 5	
12	723	50	2	Hydrochloric acid[a]	45	643 ± 5	19.3
13	923	72	4	Hydrochloric acid[a]	45	500 ± 5	
14	973	72	4	Hydrochloric acid[a]	45		7.7
15				Hydrochloric acid	45	670 ± 6	12.4
16				Hydrochloric acid	120	665 ± 5	12.8
17				Oxalic acid	60	670 ± 5	23.8
18				Oxalic acid	120		25.9

[a] Leaching after steaming.

resolution can be obtained without anisotropic quadrupolar broadening by making a correlation between the multiple and the single quantum transitions in a two-dimensional mode [21,22]. Both ^{27}Al MAS NMR and MQMAS experiments were performed on a Chemagnetics CMX Infinity 600 spectrometer (14.1 T, corresponding to ^{27}Al resonance frequency 156.3 MHz) using 2.5-mm HX MAS probe heads. Magic angle spinning (MAS) was performed at rotation frequency 25 kHz. Relaxation delays of 0.5–1 s were used to allow quantitative analysis of the spectra. MAS spectra were recorded employing single pulse excitation at 35 kHz rf-field strength and duration corresponding to $\pi/18$ pulse angle. Chemical shifts were referenced to 1 M aqueous $Al(NO_3)_3$. ^{27}Al 3QMAS shifted echo spectra were recorded from all samples using double frequency sweeps (DFS) for enhancement of triple to single quantum coherence transfer. DFSs [23,24] were generated on 25-ns steps by means of a PC-based arbitrary wave form generator from National Instruments (DAQArb PC15411) according to

$$\omega_1(t) = \omega_a \cos \int \omega_m \, dt, \quad \omega_m = \omega_s + \frac{\omega_f - \omega_s}{\tau} t,$$

with the modulated rf-field strength $\omega_1(t)$, the rf-amplitude $\omega_a(t)$, the start and final modulation frequencies $\omega_s(t)$ and $\omega_f(t)$, and the sweep duration τ. Triple quantum excitation pulses were optimized at 170-kHz rf-field strength. Diverging DFSs sweeping a frequency range from 10 to 1000 kHz within a quarter of a rotor period (10 μs) were used for triple to single quantum coherence conversion, maximizing the adiabaticity and hence the efficiency by tuning the DFS rf-field amplitude. A quality check of the DFS modulation using a spectrum analyzer proved clean modulation with carrier leakage less than 1% of the modulation rf-amplitude. The NMR parameters were determined from the ^{27}Al MQ MAS spectra. These parameters were then used to simulate the ^{27}Al MAS NMR spectra with the help of a program developed in MATLAB. Taking into account the distributions of NMR parameters, it was possible to obtain quantitative results. The isotropic chemical shifts determined from the ^{27}Al MQ MAS and ^{27}Al MAS experiments agreed well within experimental accuracy. The samples are measured under wet conditions, to minimize the chance that any aluminum is escaping detection. The spectra in this study are presented sheared.

2.4. Kinetic measurements

The catalytic activity of the Beta samples was measured batchwise for the acylation of the anisole with octanoic acid in an open reflux glass configuration. The activity measurements were performed with 50 ml of 0.2 mol/l octanoic acid in anisole, 300 mg of catalyst, a temperature of 428 K (boiling point of anisole), and atmospheric pressure. Before the catalytic performance, was measured the Beta samples were calcined in air for 4 h at 673 K to remove physisorbed water.

Activity ($l\, g_{cat}^{-1}\, h^{-1}$) was defined as the initial apparent first order rate constant k normalized for the catalyst concentration. Selectivities were calculated as the ratio of the acylated aromatic substrate *para*-octanoyl anisole and the converted octanoic acid.

3. Results

3.1. Physicochemical characteristics

The surface area characteristics of the parent Beta, as determined with nitrogen adsorption, are presented in Table 1. The samples show a surface area of 600–670 m^2/g, a micropore volume of 0.171–0.192 ml/g, and a mesopore volume of 1.03–1.23 ml/g. Treating the parent Beta with steam or an acid did not result in any significant changes in the surface area and the pore volume within the experimental error of the nitrogen adsorption technique, with one exception: treating the zeolite with acid after steaming at very high temperatures (923–973 K) results in a significant decrease of the surface area to 500 m^2/g. Bulk Si/Al ratios were measured with XRF and the results are listed in Table 1. The bulk Si/Al ratio of the parent Beta has a value of 13.0. After steaming the bulk Si/Al ratio is not altered; even in the case of 24 h of steaming the Si/Al ratio is exactly the same as the Si/Al ratio of the parent Beta (13.0). However, after the parent or steamed Beta is treated with acid, higher bulk Si/Al ratios are found. For the oxalic-acid-treated Beta the bulk Si/Al ratio increased to 51.

A TEM micrograph of the parent Beta is presented in Fig. 1. Small crystallites are visible with a particle size of 15–20 nm, which are clustered. In Fig. 1b, the TEM micrograph is shown of sample #6, which was steamed, and in Fig. 1c an oxalic acid leached sample #17. As these pictures are representative of all samples, no distinction can be made between any of the samples on the basis of TEM.

The ^{27}Al MQ MAS NMR measurement of the parent Beta is presented in Fig. 2a. The corresponding ^{27}Al MAS NMR spectrum is given on top of the MQ MAS spectrum. Tables 2a and 2b give the results of the deconvolutions of the ^{27}Al (MQ) MAS NMR spectra. In this table, it is also indicated whether whether these species are framework (FW) or not (N-FW). A typical fit is shown in Fig. 3 showing excellent agreement between data and fit. The spectrum in Fig. 2a shows two groups of peaks, at around 55 ppm and 0 ppm, which are attributed to respectively tetrahedral and octahedral coordinated aluminum. The tetrahedral peak contains the coordinations $Al(IV)_a$ and $Al(IV)_b$ characteristic of the framework of Beta [25]. These peaks have been assigned to different crystallographic T-positions. The intensity ratio of these two peaks, as given in Table 2b, indicates that the sample is dealuminated [25]. Moreover, additional peaks in the spectrum can be observed. These are called $Al(IV)_c$, Al(V), $Al(VI)_a$, and $Al(VI)_b$ and compose more than 60% of the total intensity under the spectrum (Table 2b). This aluminum could be extraframework amorphous aluminum-oxide species left over from the synthesis or it could have been formed during dealumination of the zeolite

Table 2
^{27}Al MQ MAS spectra

(a) Peak parameters as determined from spectra

Peak	Isotropic chemical shift[a] (ppm)	Quadrupolar couplings constant (MHz)
$Al(IV)_a$	61.5	2.5[b]
$Al(IV)_b$	57.5	1.9[b]
$Al(IV)_c$	61.5	6[c]
Al(V)	33	6.5[c]
$Al(VI)_a$	2.7	0.25[b]
$Al(VI)_b$	1	5[c]

(b) Relative peak intensities of spectra

Sample	Peak $Al(IV)_a$ FW[d]	Peak $Al(IV)_b$ FW	Peak $Al(IV)_c$ N-FW[e]	Peak Al(V) N-FW	Peak $Al(VI)_a$ FW	Peak $Al(VI)_b$ N-FW	Relative total intensity	Ratio $Al(IV)_a$/ $Al(IV)_b$
P	11	24	25	10	3.4	25	1.01	0.48
1	10	24	25	11	4.6	25	0.99	0.42
2	11	25	24	12	3.3	26	1.04	0.42
3	10	24	23	14	4.5	24	1.09	0.42
4	9	23	25	15	4.6	25	1	0.37
5	6	21	25	21	3.3	25	0.97	0.30
18	15.9	29.0	0	4.3	0	51	0.25	0.55

[a] ±0.5 PPM.
[b] ±0.25 MHz.
[c] ±0.75 MHz.
[d] Framework.
[e] Nonframework.

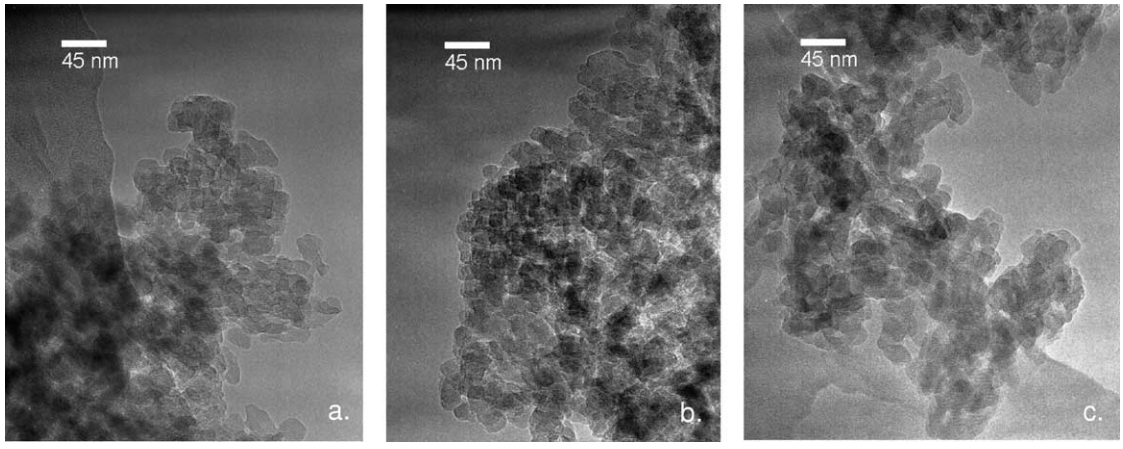

Fig. 1. TEM micrographs. (a) Parent BEA (Si/Al 12). (b) Steamed BEA #6 (723 K, 72%, 4 h). (c) Acid-leached BEA #17 (1 h, 1 M oxalic acid).

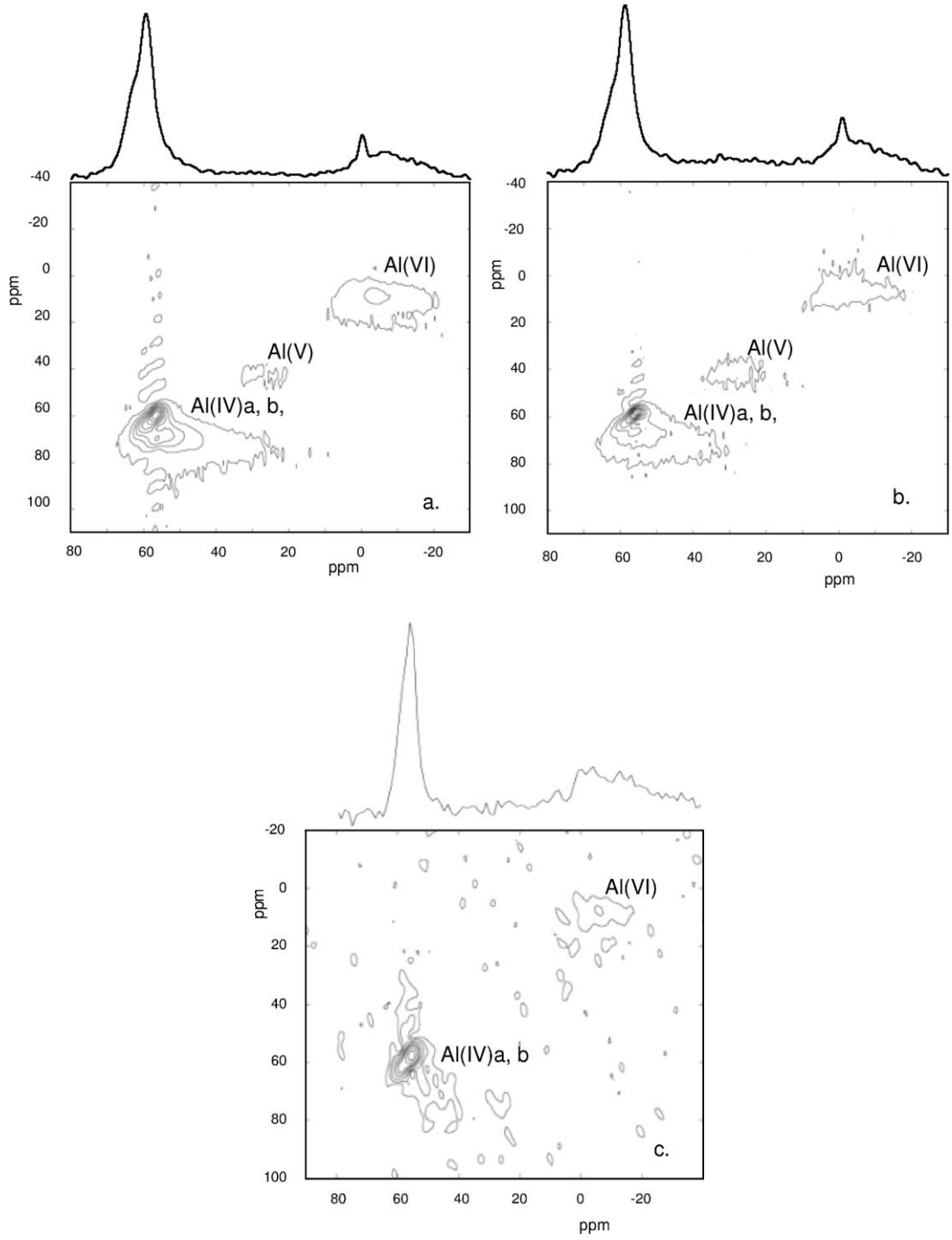

Fig. 2. (a) ^{27}Al MQ MAS NMR measurement of the parent BEA; the corresponding ^{27}Al MAS NMR spectrum is given on top. (b) ^{27}Al MQ MAS NMR measurement of the steamed BEA (673 K for 24 h in 38 vol% steam); the corresponding ^{27}Al MAS NMR spectrum is given on top. Note the increase in intensity of Al(IV)$_c$ and Al(VI). (c) ^{27}Al MQ MAS NMR measurement of the BEA treated in oxalic acid (#18); the corresponding ^{27}Al MAS NMR spectrum is given on top.

during post-synthesis treatments. It is striking that more than half the aluminum present in the spectra of the parent zeolite cannot be ascribed to framework aluminum in normal T-site positions, Al(IV)$_a$ and Al(IV)$_b$. The sharp octahedral peak represented in the spectrum by Al(VI)$_a$ has been ascribed to a framework connected octahedral aluminum, normally seen for an acidic zeolite Beta [25–27]. Fig. 2b depicts the result after the parent Beta is steamed for 24 h at 673 K with a steam content of 38 vol%. The ^{27}Al MQ MAS NMR spectrum of this sample is similar to the spectrum of parent Beta (Fig. 2a), but reveals changes in relative intensity of the peaks in the spectra (Table 2b). No new peaks were observed after the treatment. The spectra of the Beta after 1, 2, and 10 h of steaming are not shown but the changes from parent

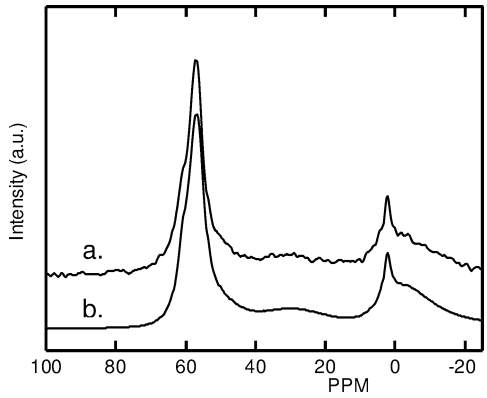

Fig. 3. Example of a NMR spectrum and the corresponding fit (sample #3, steamed at 673 K, 38 vol% steam for 3 h). (a) NMR spectrum as measured. (b) Corresponding fit.

to 24 h steaming are continuous, as visible in Table 2b. It is clear that the oxalic acid treated sample shows a complete removal of $Al(IV)_c$ and a large loss in intensity of peak Al(V). The total intensity under the spectrum is largely diminished, which is indicative of removal of aluminum from the sample, also shown by the XRF measurements (Table 1). Interestingly, the intensity ratio of peaks $Al(IV)_a$ and $Al(IV)_b$ for the oxalic acid leached sample (#18) is increased compared to the parent sample (Table 2). The steaming caused the ratio to decrease by preferential dealumination of species $Al(IV)_a$. Clearly, the dealumination with oxalic acid results in the loss of framework aluminum at different crystallographic positions than by steaming.

XRD (not shown) showed that the crystallinity of the samples was largely preserved after the different treatments. Small differences in relative peak intensities was observed. Steaming of the parent Beta (Si/Al 13) at 673 K with varying times (1–24 h) and for 4 h at various temperatures up to 973 K did not result in any significant loss of crystallinity.

3.2. Performance in the acylation reaction

In the acylation of anisole with octanoic acid (0.2 mol/l octanoic acid in anisole at 428 K), the parent Beta exhibits an activity of $0.03\,l\,g^{-1}\,h^{-1}$, which is comparable to that of FAU zeolite and the Nafion–silica composite SAC13 (12). The activity of USY is significantly lower, and that of MFI was negligible [12]. The selectivity of the parent Beta towards the desired *para*-acylated anisole is 80% at 50% conversion. The side products are phenol, methylated octanoic acid, and paraacylated phenol. These products are formed in approximately equal amounts and result from reaction of the octanoic acid with the methoxygroup of anisole. All selectivities remain constant as a function of the conversion, which indicates the presence of parallel side reactions.

The good activity and selectivity of zeolite Beta could be further enhanced by acid leaching and steaming. This is depicted in Fig. 4. Steaming the parent zeolite at 673 K (38 vol% steam) only leads to higher activity for steaming

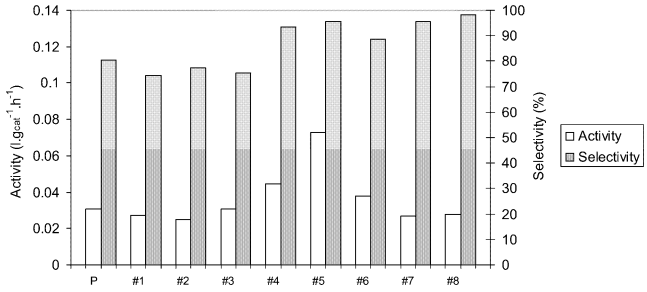

Fig. 4. The effect of steaming BEA on the activity and selectivity in the acylation of anisole with octanoic acid, as measured under standard conditions (0.2 mol/l, 428 K, 0.6 wt% catalyst). The numbers on the *x*-axis correspond to the catalyst numbers in Table 1.

longer than 3 h. After 1–3 h, the activity is maintained, or even drops slightly, but after 10 h of steaming the activity increases 50% and after 24 h an increase of 140% is observed.

Clearly, after steaming for periods longer than 3 h, an increase in activity is accompanied by an increase in selectivity for samples steamed under the milder conditions (38% steam). The selectivity drops slightly at steaming times of 1–3 h, but increases to 95% after 10 and 24 h of steaming. Increasing the steaming temperature to 723 K and the steam content to 72% results in an increase of 25% in the activity, and a slightly higher selectivity of 88%. At higher temperatures, even up to 973 K, the original activity is maintained, but the selectivity is increased to 98%.

The effect of leaching after steaming on the acylation activity and selectivity is depicted in Fig. 5. Globally, the hydrochloric acid leaching after steaming does not have a positive effect on the activity, except for the sample that was first steamed for 1 h at 673 K. Here, an increase in the activity after leaching was obtained. For samples steamed at higher steam contents (72%) and high temperatures (923 K), the activity even decreased.

The effect of treating the parent Beta in hydrochloric acid and oxalic acid on the acylation activity and selectivity is depicted in Fig. 6. Treatment in hydrochloric acid (1 M)

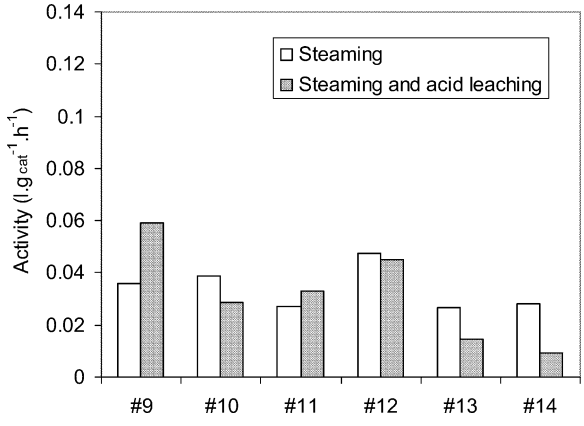

Fig. 5. The effect of acid leaching after steaming Beta on its activity in the acylation of anisole with octanoic acid, as measured under standard conditions (0.2 mol/l, 428 K, 0.6 wt% catalyst).

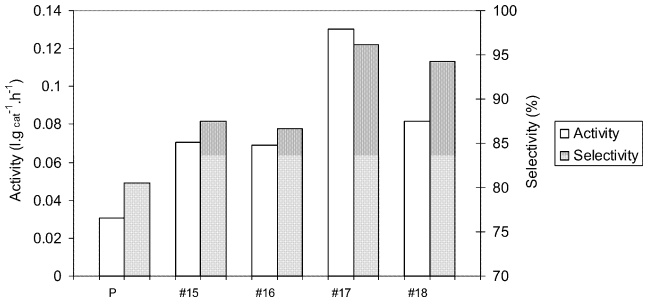

Fig. 6. The effect of acid leaching of BEA on its activity and selectivity in the acylation of anisole with octanoic acid, as measured under standard conditions (0.2 mol/l, 428 K, 0.6 wt% catalyst).

for 45 or 120 min results in an increase in the activity by a factor of 2. Treating time does not affect activity between 45 and 120 min. Treatment of Beta in 1 M oxalic acid for 60 min results in an increase in the activity by a factor of 4. Longer leaching results in activity slightly lower than for the 60-min-leached Beta. The selectivity is improved for both acid treatments, especially for oxalic acid where an increase from 80 to 95% is observed.

It has been mentioned in the literature [28] that enhancement of the performance of zeolites after steaming and acid leaching could be due to migration of the extra framework aluminum into the reaction mixture, hereby acting as a homogeneous catalyst. Therefore, leaching of the active species was studied by filtering the hot reaction mixture for a steamed Beta, an acid leached sample after steaming, and a hydrochloric acid leached sample. In all cases, the reaction did not continue after hot filtration, indicating that no active species had leached from the solid catalyst during reaction conditions.

4. Discussion

In general, it can be stated that steaming (longer than 24 h, higher temperatures, and higher steam content) and acid treatment lead to an increase in activity and selectivity. For the acid treatment, oxalic acid is the most effective. Acid leaching after steaming has no effect. The Beta structure is not significantly affected by especially harsh steaming conditions, as follows from XRD, TEM, and BET analysis. This shows that the starting sample has a high stability, which is not a priori expected from zeolite Beta (vide infra).

The most significant changes are observed by ^{27}Al MQ MAS NMR measurements, which give information about the type and coordination of the aluminum in the samples. So any change due to the applied treatment must be one of a very local modification.

The parent Beta used in this study already shows the presence of a significant amount of extraframework aluminum. Moreover, the relative intensity ratio of peaks $Al(IV)_a$ and $Al(IV)_b$ as shown by the ^{27}Al (MQ) MAS spectra (Fig. 2 and Table 2b) of this material is characteristic of a dealuminated Beta zeolite [25]. From other zeolite structures, such as UltraStableY, it is well known that dealumination stabilizes the structure of the zeolite which is paralleled with a higher activity [13]. The high content of amorphous aluminum-(silicon-) oxide species present in the parent Beta sample is probably caused by the in situ steaming during the calcination in the production process [16]. The dealumination caused by this in situ steaming process could explain the high stability of the starting material towards steam and mineral acids. The commercial processes of synthesizing zeolite beta are based on the process described in the first patent about zeolite beta which was published in 1967 by Wadlinger et al. [29]. First, a synthesis mixture is prepared which contains a silicon source, a source of aluminum, water, and a template (often triethanolamine). This synthesis mixture is crystallized under hydrothermal conditions for 6–8 days at a temperature of about 140–150 °C. In the process, the zeolite crystals are formed. After washing, the template is burned off by calcination at relative high temperatures (200–800 °C). During this calcination process, is very plausible that steam has formed and that this steam can already dealuminate the beta zeolite structure. Moreover, as the zeolite was obtained from the supplier in an acid form, and it is not known which method was used to convert the zeolite into the acid form, of course this kind of aftertreatments can also affect the amount of dealumination of the zeolite structure.

Steaming the parent Beta at 673 K for 1 to 24 h does not result in the formation of new aluminum species, but results in an increase in intensity of peaks $Al(IV)_c$, Al(V), and $Al(VI)_b$ relative to the two normal framework tetrahedral peaks, $Al(IV)_a$ and $Al(IV)_b$, as measured by ^{27}Al MQ MAS NMR. The decrease in activity at shorter steaming times can be explained by the formation of extraframework aluminum that blocks active sites. Pores are not plugged, because no change is observed in the surface area characterisation with nitrogen adsorption.

The dominant process during the steaming treatment is the loss of a small part of the framework tetrahedral aluminum represented by peaks $Al(IV)_a$ and $Al(IV)_b$ and a clustering of extraframework aluminum species into amorphous aluminum–(silicon)–oxidic species. This process preserves the pore topology and crystallinity of the zeolite as shown by XRD, TEM, and nitrogen physisorption (Table 1, Fig. 1). To illustrate the aspect of clustering resulting in a preserved pore topology and crystallinity, a schematic view is given in Fig. 7, in which the beta zeolite structure is depicted with the parent situation in the left pore and the situation after treatment in the right pore. The stars represent a schematic view of the active sites, becoming more accessible after clustering of the extraframework aluminum at the outer surface of the crystallites.

Dealumination by steaming leads to a further decrease in ratio of intensity of tetrahedral framework peaks $Al(IV)_a$ and $Al(IV)_b$, indicating that steaming causes preferential dealumination at specific crystallographic T-sites in zeolite Beta as observed earlier [25]. In contrast, acid leaching with

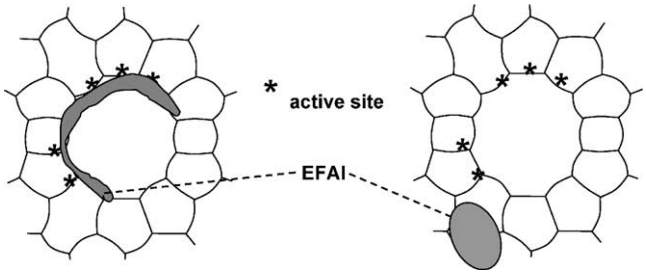

Fig. 7. A schematic view of the Beta zeolite structure in which the aspect of clustering after steaming and leaching treatment is illustrated. The parent situation is depicted in the left pore and the situation after treatment in the right pore. The stars represent a schematic view of the active sites, which become more accessible after clustering of the extraframework aluminum. As a consequence, both rate and selectivity go up, due to the higher contribution of selective sites in the pores of the crystallites.

oxalic acid results in an increase in the intensity ratio of the two normal framework peaks, indicating that different aluminum atoms are removed from the framework by acid leaching than by steaming. Clearly, a different mechanism of dealumination occurs during both treatments.

The improvement of both the activity and selectivity after steaming for periods longer than 3 h cannot be ascribed to the formation of mesopores because TEM and texture analysis did not reveal any changes in surface area or micro- or mesoporosity. Also, XRD did not show any significant changes. From the XRF analysis it is demonstrated that the aluminum is not removed from the zeolite after steaming, so only the coordination is changed. Indeed, the ^{27}Al MQ MAS NMR measurements show an increase in intensity of the amorphous aluminum oxidic species.

The activity is not significantly affected by acid treatment after steaming. Only in one case was an increase in the activity found. The reason for this increase could be the removal of the extraframework aluminum that was formed on the zeolitic structure by steaming, as XRF analysis revealed (Table 1). In this way, previously blocked acid sites can become accessible.

Leaching the parent Beta in hydrochloric and oxalic acid resulted in high activities. Especially in the case of oxalic acid, the activity is highly increased. Leaching the parent Beta in hydrochloric and oxalic acid causes aluminum to be removed from the samples, as indicated by XRF (Table 1) by the higher bulk Si/Al ratio and confirmed by the loss in signal in the ^{27}Al MAS NMR spectra (Table 2). Aluminum is effectively removed from the zeolite by oxalic acid due to its complexation properties. The ^{27}Al MQ MAS NMR spectrum reveals a clear decrease of the Al(V) peak and complete removal of $Al(IV)_c$ from the sample. Clearly, not all the octahedrally coordinated aluminum can be removed, and the tetrahedrally coordinated aluminum that is removed is not active in the acylation reaction.

It is also possible that an amorphous silica–alumina (ASA) phase could have been formed during steaming from the reaction between the extracted Si and Al [30,31]. However, as ASA (a commercial sample with a Si/Al of 0.67, BET of 425 m^2/g, pore volume of 0.67 ml/g) does not show any activity in this acylation activity [32], it is very unlikely that an amorphous silica–alumina phase is involved in the acylation activity. Moreover, it was concluded earlier in this paper that the activity increase is correlated with the effective removal of extraframework aluminum, which also confirms that the activity of the zeolite is not correlated with the extraframework aluminum, but with the activity of the zeolite structure itself.

4.1. Origin of the acylation activity

In the literature, it is not very clear whether Brønsted or Lewis sites are responsible for the acylation reaction. Of course, the ability of strong Brønsted sites to catalyze the acylation reaction is demonstrated by the high performance of the ion-exchange resin Nafion, which does not contain Lewis sites to catalyze the reaction [12]. Due to this Brønsted type behavior, it is easily thought that in zeolite Beta, Brønsted acid sites are responsible for the catalytic activity in the acylation reaction. However, it cannot be ruled out that the aluminum in the zeolite acts as a Lewis type of active site. Recently, reports suggesting the Lewis acidity of the framework in zeolites have appeared [5,33–36]. Many reports have discussed the transformation of tetrahedrally coordinated aluminum into a octahedral coordination in acidic zeolite Beta, which can be seen as Lewis activity on the framework. Indeed, it has been suggested by Haouas et al. [35] that the activity of the nitration of toluene is associated with the flexibility of the framework in zeolite Beta. According to the authors, a reversible transformation occurs of the tetrahedrally coordinated aluminum into octahedrally coordinated aluminum, forming a complex with the reactant. A similar tetrahedral–octahedral transformation of framework aluminum has been suggested to be responsible for activity in the Meerwein–Ponndorf–Verley (MPV) reaction of 4-tert-butylcyclohexanone to *cis*-4-tert-butylcyclohexanol [33]. Our study shows that the origin of the active sites should indeed be sought in the framework aluminum, as the "clean" zeolite structure, obtained after leaching with oxalic acid, gave the highest activity. The Lewis acid behavior of the tetrahedral framework aluminum might therefore be responsible for the activity in acylation reactions.

4.2. Catalytic performance

Dealumination of zeolite Beta results in a higher activity in the acylation of anisole with octanoic acid. This process is accompanied by the formation of extraframework aluminum in the case of steaming and by the removal of extraframework material from the sample by acid leaching and complexation by oxalic acid. The highest enhancement is obtained in the latter case.

Both steaming and acid leaching lead to the same effect: enhancement of the activity and selectivity. At this point,

some possible explanations can be given. Either additional active sites that have been formed or more sites that have become accessible participate in the reaction, or the active sites have become more active. Because steaming results in the formation of extraframework aluminum and acid leaching in the removal of extraframework aluminum, it seems more likely that the activity enhancement is due to the increased accessibility or participation of active sites, rather than the formation of additional active species. Some active sites may have been blocked by extraframework aluminum. Removal of this "site-blocking" aluminum (by acid leaching) results in more active sites that are accessible. In addition, any debris in the pores of the zeolite may hamper diffusion of the reactants through the pores of the zeolite. Removal of this debris then (partly) alleviates diffusional limitations.

By steaming and acid treatment, the extraframework aluminum species become mobile and are transported through the zeolite lattice. As a result of clustering of the extraframework aluminum during severe steaming the accessibility of the active sites can thus be increased (Fig. 7). Note that the pore topology remains the same after the steaming treatment, so only the active sites become more accessible within the pores. This also explains why leaching after steaming does not result in any activity enhancement, because active sites have already been made accessible by the steaming procedure.

An increase in activity after leaching and steaming is paralleled by an increase in selectivity. The removal or clustering of extraframework aluminum results in clean pores that induce the *para*-selectivity of the acylation of anisole with octanoic acid. The higher contribution of selective sites in the pores of the crystallites yields the higher selectivities.

5. Conclusions

The parent Beta, as obtained from Zeolyst International, contains large amounts of aluminum that cannot be ascribed to normal framework tetrahedral aluminum, and it shows characteristics of dealumination. This is also indicated by the high stability toward steam of the sample, ascribed to in situ dealumination during the production process. Steaming the parent Beta leads to increased activity at steaming times longer than 3 h (at 673 K). This steaming procedure leads to a change in aluminum coordinations in the sample, as was demonstrated with ^{27}Al MQ MAS NMR. Treatment in acid after steaming does not affect the texture properties of the zeolite, as was demonstrated with nitrogen adsorption and TEM. Also, the activity in the acylation reaction is not significantly affected. Leaching the parent Beta in hydrochloric and oxalic acid results in high activities, especially in the case of oxalic acid. This acid treatment leads to removal of the distorted tetrahedrally and pentacoordinated aluminum. After hot filtration the reaction did not continue, indicating that no active species will leach from the zeolite during reaction conditions.

The improvement of both the activity and selectivity after steaming for periods longer than 3 h is most likely due to enhanced participation of the active sites: steaming clusters extraframework aluminum and acid leaching removes this extraframework aluminum, improving accessibility. This may also explain the increased selectivity due to the lower chance of side reactions.

Acknowledgments

The NMR facility at Nijmegen University, The Netherlands, is kindly thanked for providing magnetic measurement time. Dr. H. Schaefer is thanked for his help during the measurements. Dr. P.L.J. Kooyman of the National Centre for High Resolution Microscopy, Delft University of Technology, the Netherlands, is kindly acknowledged for performing the electron microscopic investigations. J. Groen, J. Padmos, and N. van der Pers, also from Delft University of Technology, are acknowledged for performing the texture analysis, XRF, and XRD measurements, respectively.

References

[1] W.F. Hölderich, H. van Bekkum, Stud. Surf. Sci. Catal. 58 (1991) 631.
[2] F. Kapteijn, J.J. Heiszwolf, T.A. Nijhuis, J.A. Moulijn, CATTECH 3 (1999) 24.
[3] A. Corma, M.J. Climent, H. García, J. Primo, Appl. Catal. 49 (1989) 109.
[4] G. Harvey, A. Vogt, H.W. Kouwenhoven, R. Prins, in: Proc. Int. Zeol. Conf., 9th, 1993, p. 363.
[5] U. Freese, F. Heinrich, F. Roessner, Catal. Today 49 (1999) 237.
[6] H.K. Heinichen, W.F. Hölderich, J. Catal. 185 (1999) 408.
[7] E.A. Gunnewegh, A.J. Hoefnagel, H. van Bekkum, Stud. Surf. Sci. Catal. 97 (1996) 447.
[8] B. Chiche, A.F. Finiels, C. Gauthier, P. Geneste, J. Graille, D. Pioch, J. Org. Chem. 51 (1986) 2128.
[9] B. Chiche, A.F. Finiels, C. Gauthier, P. Geneste, Appl. Catal. 30 (1987) 365.
[10] C. Gauthier, B. Chiche, A.F. Finiels, P. Geneste, J. Mol. Catal. 50 (1989) 219.
[11] M. Spagnol, L. Gilbert, H. Guillot, P.J. Tirel, WO Patent WO 97/48665, 1997. Assigned to Rhone-Poulenc Chimie, France.
[12] A.E.W. Beers, I. Hoek, T.A. Nijhuis, R.S. Downing, F. Kapteijn, J.A. Moulijn, Top. Catal. 13 (2000) 275.
[13] R.A. Beyerlein, C. Choi-Feng, J.B. Hall, B.J. Huggins, G.J. Ray, in: Fluid Catalytic Cracking III, 1994, p. 81.
[14] J.J. Lazaro Munoz, A. Corma Canos, J.M. Frontela Delgado, US Patent US5057471, 1991.
[15] M. Müller, G. Harvey, R. Prins, Micropor. Mesopor. Mater. 34 (2000) 135.
[16] P.J. Kunkeler, B.J. Zuurdeeg, J.C. van der Waal, J.A. van Bokhoven, D.C. Koningsberger, H. van Bekkum, J. Catal. 180 (1998) 234.
[17] B. Janssens, Zeolites as Alternative Catalysts for Friedel–Crafts Alkylation and Acylation Reactions, PhD thesis, Katholieke Universiteit Leuven, Belgium, 1996.
[18] P. Moreau, A. Finiels, P. Meric, J. Mol. Catal. A Chem. 154 (2000) 185.

[19] E.G. Derouane, C.H. Dillon, S.B. Derouane-Abd Hamid, J. Catal. 187 (1999) 209.
[20] D. Rohan, C. Canaff, E. Fromentin, M. Guisnet, J. Catal. 177 (1998) 296.
[21] L. Frydman, J.S. Harwood, J. Am. Chem. Soc. 117 (1995) 5367.
[22] A. Medek, J.S. Harwood, L. Frydman, J. Am. Chem. Soc. 117 (1995) 12779.
[23] A.P.M. Kentgens, R. Verhagen, Chem. Phys. Lett. 300 (1999) 435.
[24] D. Iuga, H. Schäfer, R. Verhagen, A.P.M. Kentgens, J. Magnet. Reson. 147 (2000) 192.
[25] J.A. van Bokhoven, D.C. Koningsberger, P. Kunkeler, H. van Bekkum, A.P.M. Kentgens, J. Am. Chem. Soc. 122 (2000) 12842.
[26] L.C. de Ménorval, W. Buckermann, F. Figueras, F. Fajula, J. Phys. Chem. 100 (1996) 465.
[27] E. Bourgeat-Lami, P. Massiani, F. Di Renzo, P. Espiau, F. Fajula, F. des Courières, Appl. Catal. 72 (1991) 139.
[28] R. Fang, G. Harvey, H.W. Kouwenhoven, R. Prins, Appl. Catal. A General 130 (1995) 67.
[29] R.L. Wadlinger, G.T. Kerr, L. Township, E.J. Rosinksi, US Patent 3308069, 1967.
[30] J. Sanz, V. Fornés, A. Corma, J. Chem. Soc. Faraday Trans. I 84 (1988) 3113.
[31] A. Omegna, M. Haouas, A. Kogelbauer, R. Prins, Micropor. Mesopor. Mater. 46 (2001) 177.
[32] Unpublished data, measured by the author at the laboratory of the Delft University of Technology.
[33] J.A. van Bokhoven, D.C. Koningsberger, P. Kunkeler, H. van Bekkum, J. Catal., in press.
[34] G.H. Kuehl, H.L.C. Timken, Micropor. Mesopor. Mater. 35–36 (2000) 521.
[35] M. Haouas, A. Kogelbauer, R. Prins, Catal. Lett. 70 (2000) 61.
[36] G.L. Woolery, G.H. Kuehl, H.C. Timken, A.W. Chester, J.C. Vartuli, Zeolites 19 (1997) 288.